Analysis of Artificial Dielectric Lens with Metallic Rectangular Chips for Terahertz Wave Band and Physical Explanation by Periodic Model

Takehito Suzuki[1*], Tomonari Suzuki[1], John C. Young[2], Keisuke Takano[3], Hideaki Kitahara[3], Masanori Hangyo[3]

[1]Department of Electrical & Electronic Engineering,
Ibaraki University, 4-12-1 Nakanarusawa, Hitachi, Ibaraki 316-8511, Japan
[2]Electrical and Computer Engineering, University of Kentucky, Lexington, Kentucky 40506-0046, USA
[3]Institute of Laser Engineering, Osaka University, 2-6 Yamadaoka, Suita, Osaka 565-0871, Japan
*corresponding author, E-mail: takehito@hcs.ibaraki.ac.jp

Abstract

Optical devices for the terahertz wave band are being developed now and require better designs. This paper analyzes an artificial dielectric lens with metallic rectangular chips for the terahertz wave band. This paper also provides an explanation of the phenomena by use of a periodic model. The periodic analysis model, extracted from the full one by assuming periodicity, confirms the phase delay as the mechanism that produces the focusing effect. Furthermore, the results of full model confirm the focusing length is longer with the larger periodicity of rectangular metal chips along the direction transverse to the propagation direction. It also indicates a nonuniform change for the periodicity along the propagation direction and the longer focusing length with narrower rectangular chips. The results of the full model analysis are qualitatively consistent with those of the periodic model one. This implies that the design for an exact size lens is possible through use of the periodic model.

1. Introduction

Optical devices for the terahertz wave band ranging from 0.1 to 10 THz are currently being developed and require improved designs. It is not easy to realize an arbitrary refractive index n using naturally-occurring materials. When materials are directly used for optical devices, the material properties themselves determine the optical characteristics. Typical lenses for the terahertz wave band are made of high density polymer, Tsurupica, and silicon with refractive indices of 1.52, 1.56, and 3.41, respectively. It is significant that the unit cell of the electromagnetic metamaterial controls the refractive index with respect to design flexibility and cost performance. Lenses composed of electromagnetic metamaterials, sphere arrays, disk arrays, square plate arrays, and strip arrays, have been proposed for microwave frequency band in [1]-[5]. These lenses produce focusing action due to the phase delay, slow wave effect. Lenses that use the high phase velocity of the propagation mode in a parallel plate waveguide structure have been proposed in [6]. The works in [7]-[10] present a metamaterial absorber, that in [11] presents an antireflection coating, that in [12] presents a metamaterial with an unnaturally high refractive index, and that in [13] and [14] present a three-dimensional metamaterial in the terahertz wave band. The effective permittivity and permeability of a metal slit array are derived and the proper refractive index is estimated as 1 in [15]. The work in [16] reports anomalies in a double-layered metallic slit. It is relatively easy to fabricate a terahertz-band metamaterial by metallic processing and chemical reduction on a film with thin metal [13], [14] compared to a metamaterial in optical range because the

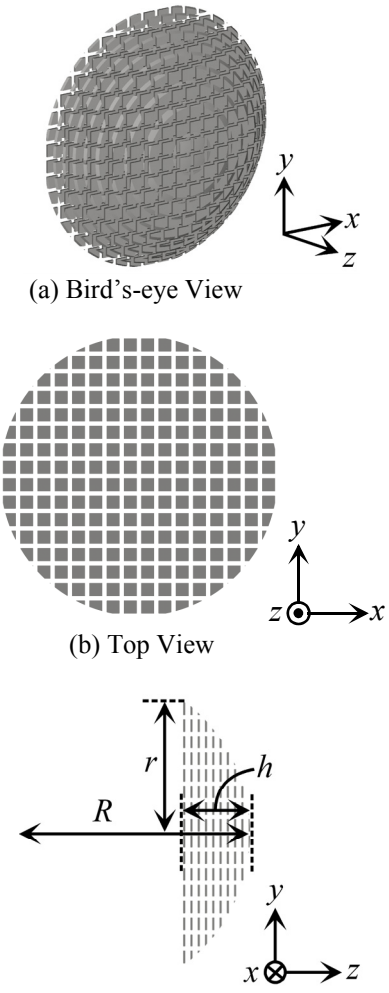

Figure 1: Lens of rectangular metallic chips for terahertz wave band

dimensions of the unit element are on the order of tens of microns.

This paper presents the focusing effect of an artificial dielectric lens with metallic rectangular chips in the terahertz wave band and operational explanation of the focusing length through use of a periodic analysis model. The periodic analysis model, which is extracted from the full model by assuming periodicity, confirms the phase delay used to estimate the focusing effect in the full model. Commercial EM simulators are now quite powerful but are still computationally heavy for the design and optimization of a whole array. A lens with a large but finite and complicated unit cell array is generally cumbersome and challenging to design. The work in [2] comments the necessity of further publication for an explanation of the lens operation. The analysis and design using the periodic model is fast and effective and can be used in an iterative design procedure [15]. An HFSS simulation of the full model confirms that the focusing length is longer with the larger periodicity of rectangular metal chips along the direction transverse to the propagation direction. It also confirms a nonuniform change for the periodicity along the propagation direction and the longer focusing length with narrower rectangular chips. These phenomena are demonstrated by the periodic analysis model. Results from the periodic model imply the possibility of efficient design for a full size lens. The dimensions of the full model in the analysis are small compared with those of the actual lens to reduce analysis time. Section 2 explains the structure and dimensions of artificial dielectric lens with metallic chips. Section 3 shows the analysis results of the periodic model and Section 4 shows those of full model.

2. Artificial dielectric lens with metallic rectangular chips

Figure 1 shows the artificial dielectric lens with metallic rectangular chips. A $+z$ traveling TEM wave with a x-polarized electric field propagates through the lens. For a true dielectric material, the phase of electromagnetic wave in the dielectric material is delayed by the slow-wave effect. This effect is caused by the molecules and atoms in the dielectric material acting as electrical dipoles to the electromagnetic wave. Thus, the lens shape focuses the electromagnetic wave. In the metallic lens, each of the rectangular metallic chips macroscopically acts as an electrical dipole and the behavior is similar to a dielectric material. The lens dimensions, r=1.32 mm (2.21λ), R=1.60 mm (2.67λ) and h=0.70 mm (1.17λ), are used for the full model analysis. Figure 2 shows the unit cell models. Pattern A focuses on the characteristics for periodicity of rectangular metal chips along the direction transverse to the propagation direction. Pattern B focuses on the characteristics for the periodicity along the propagation direction. Pattern C focuses on the characteristics for the rectangular chip size. The spacing of adjacent rectangular chips is fixed with 40 μm (0.067λ) in Pattern C. Table 1 shows the parameters of the reference model in Fig. 2. The design frequency is 0.5 THz.

3. Phase delay analysis by periodic model

Figure 3 shows the periodic analysis model extracted from the full model. The phase delay is derived from the analysis of the periodic model in Fig. 3. Figure 4 shows the phase delay results by Ansys HFSS (Ver. 13).

The dimensions of periodicity p_x and p_y in Pattern A are p_x=p_y=160 μm (0.27λ), 200 μm (0.33λ), 240 μm (0.40λ). The delayed phases at the 10th chip are -255.3, -159.4 and -108.3 degrees with p_x=p_y=160 μm, 200 μm and 240 μm, respectively, as shown in Fig. 4 (a). The phase delay decreases as the periodicity p_x and p_y increase.

The dimensions of p_z in Pattern B are p_z=30 μm (0.050λ), 70 μm (0.12λ), 110 μm (0.18λ). The delayed phases at the output edge are -209.9, -255.3 and -191.4 degrees with p_z=30 μm, 70 μm and 110 μm, respectively, as

Reference Model	Pattern A	Pattern B	Pattern C
Parameters	Length p_x Length p_y	Width p_z	Length a Length b
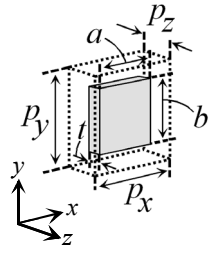	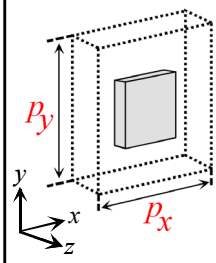	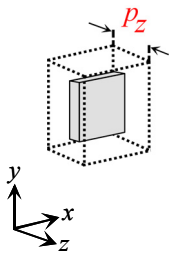	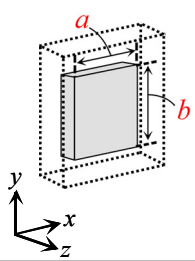
Table 1	A-1 p_x=200 μm, p_y=200 μm	B-1 p_z =30 μm	C-1 a =80 μm, b =80 μm
	A-2 p_x=240 μm, p_y=240 μm	B-2 p_z =110 μm	C-2 a =160 μm, b =160 μm

Figure 2: Unit cell models

shown in Fig. 4 (b). The length of horizontal axis in Fig. 4 (b) is normalized by wavelength. The phase delay changes nonuniformly with the periodicity p_x and p_y. These phenomena may be caused by the standing wave between the metal chips. The phase delay from p_z=30 μm to p_z=190 μm changes with periodicity, even though that from p_z=190 μm to p_z=230 μm does not change with periodicity. The dimensions of periodicity a and b in Pattern C are a=b=80 μm (0.13λ), 120 μm (0.20λ), 160 μm (0.27λ). The delayed phase at the 10th chip are -155.3, -255.3 and -391.1 degrees with a=80 μm, 120 μm and 160 μm, respectively, as shown in Fig. 4 (c). The phase delay increases as the chip size a and b increase.

The decreasing phase delays imply a decreasing of refractive index, which results in an increasing of the focusing length.

4. Lens full model analysis

Only one quarter of the analysis model is analyzed using image theory [16] in order to reduce the problem size. The full wave analysis results are obtained by Ansys HFSS (Ver. 13). The workstation CPU is an Intel Xeon 5690 (3.46 GHz 6 Core) x 2 and applied memory is 129 GB. It took 26 hours 23 minutes to analyze the reference model. The incident electric field is shown in Figure 5 for the reference model. It is verified that the lens with rectangular metallic chips produces a focusing effect. The local maximum value of the electric field magnitude is 3.6 times that of the incident wave at 1.12 mm (3.03λ) from the top of lens sphere.

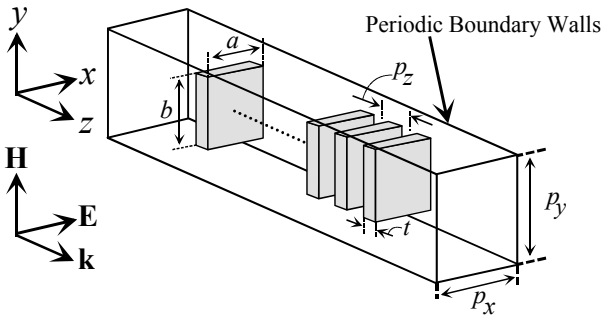

Figure 3: Analysis model with periodic boundary walls for estimation of phase delay.

Table 1: Lens parameters for reference model.

a	120 μm(0.20λ)
b	120 μm(0.20λ)
t	20 μm(0.033λ)
p_x	160 μm(0.27λ)
p_y	160 μm(0.27λ)
p_z	70 μm(0.12λ)

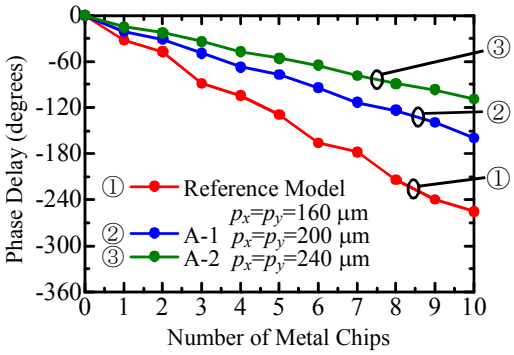

(a) Pattern A

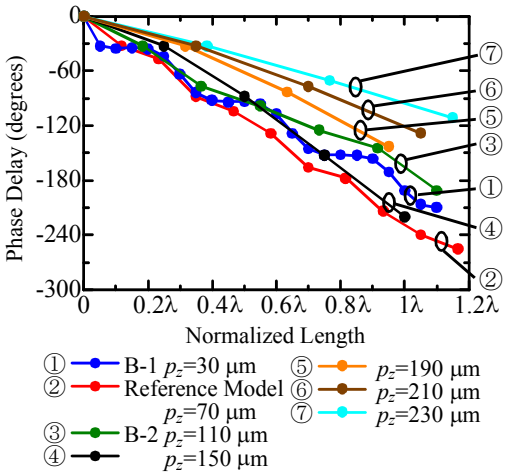

(b) Pattern B

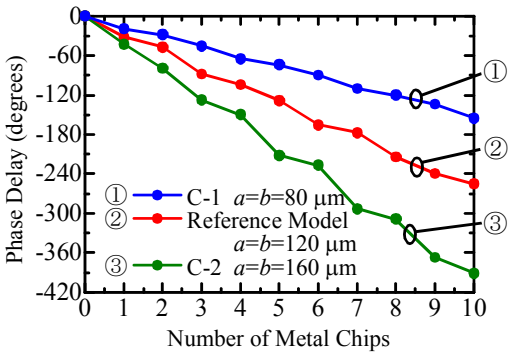

(c) Pattern C

Figure 4: Phase delay for analysis model with periodic boundary walls.

4.1. Pattern A

Figure 6 (a) shows the full model analysis result for Pattern A-1, p_x=p_y=200 μm (0.33λ). For Pattern A-1, the local maximum value of the electric field magnitude is 3.0 times that of the incident wave at 1.89 mm (3.15λ) from the top of the lens sphere, as shown in Figure 9 (b). Fig. 6 (b) shows the full model analysis result for Pattern A-2, p_x=p_y=240 μm (0.40λ). For Pattern A-2, the local maximum value of the electric field magnitude is 2.4 times that of the incident wave at 2.25 mm (3.75λ) from the top of the lens sphere, as shown in Fig. 9 (b). The periodic model results in

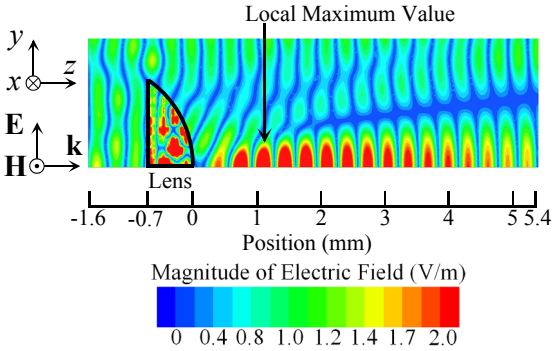

Fig. 5 Full wave analysis results for reference model.

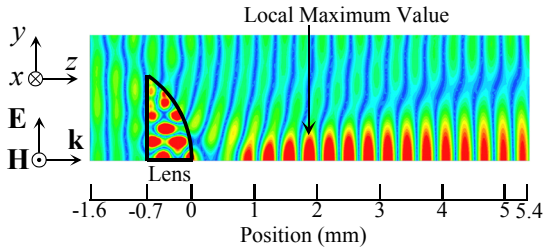

(a) A-1 p_x= p_y=200 μm (0.33λ)

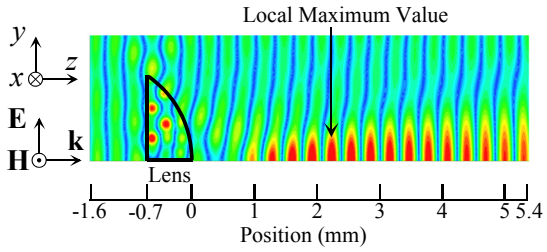

(b) A-2 p_x= p_y=240 μm (0.40λ)

Figure 6: Full wave analysis results for pattern A.

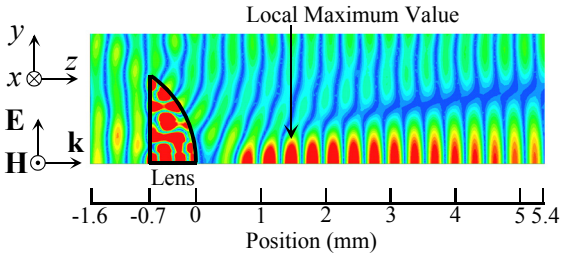

(a) B-1 p_z=30 μm (0.050λ)

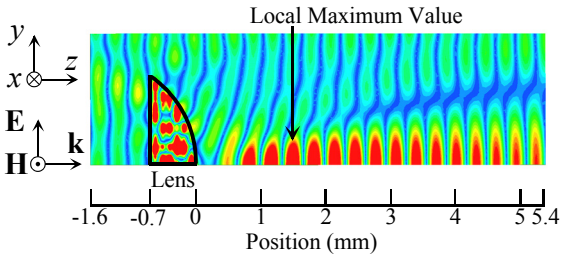

(b) B-2 p_z=110 μm (0.18λ)

Figure 7: Full wave analysis results for pattern B.

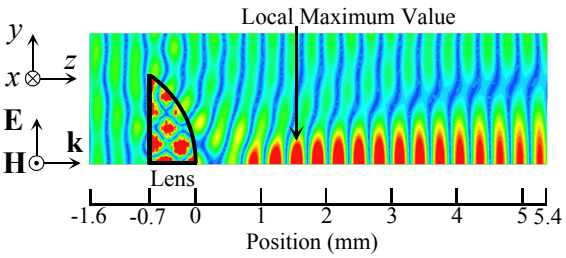

(a) C-1 a=b=80 μm (0.13λ)

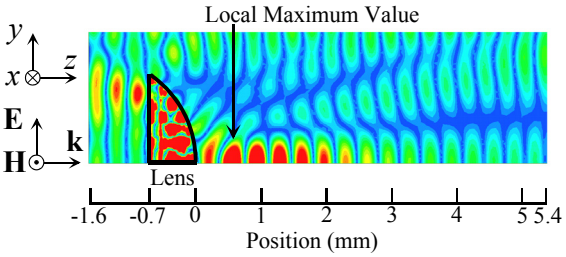

(b) C-2 a=b=160 μm (0.27λ)

Figure 8: Full wave analysis results for pattern C.

Fig. 4 (a) are qualitatively consistent with those of full model because the focusing length increases as the periodicity p_x and p_y increases. The equivalent refractive index decreases as the periodicity p_x and p_y increases.

4.2. Pattern B

Figure 7 (a) shows the full model analysis result for Pattern B-1, p_z=30 μm (0.050λ). For Pattern B-1, the local maximum value of the electric field magnitude is 3.0 times that of the incident wave at 1.49 mm (2.48λ) from the top of the lens sphere, as shown in Fig. 9 (b). Fig. 7 (b) shows the full model analysis result for Pattern B-2, p_z=110 μm (0.18λ). For Pattern B-2, the local maximum value of the electric field magnitude is 3.4 times that of the incident wave at 1.50 mm (2.50λ) from the top of the lens sphere, as shown in Fig. 9 (b). The phase delay for p_z=30 μm exists between that for p_z=70 μm and p_z=110 μm, as shown in Fig. 4 (b). Fig. 4 shows a nonuniform change for the periodicity along the propagation direction and a longer focusing length with narrower rectangular chips. The periodic model results shown in Fig. 4 (b) are qualitatively consistent with those of full model because the focusing length for p_z=30 μm exists between that for p_z=70 μm and p_z=110 μm, as shown in Fig. 9 (b). This suggests we can simplify the design of unit cell array with exact size to an iterative one by using a periodic model, even under nonuniform changes with parameters.

4.3. Pattern C

Figure 8 (a) shows the full model analysis result for Pattern C-1, a=b=80 μm (0.13λ). For Pattern C-1, the local maximum value of the electric field magnitude is 3.0 times that of the incident wave at 1.57 mm (2.62λ) from the top of the lens sphere, as shown in Fig. 9 (c). Fig. 6 (b) shows the full model analysis result for Pattern C-2, a=b=160 μm (0.27λ). For Pattern C-2, the local maximum value of the

electric field magnitude is 4.0 times that of the incident wave at 0.59 mm (0.98λ) from the top of the lens sphere, as shown in Fig. 9 (c). The results of periodic model in Fig. 4 (c) are qualitatively consistent with those of full model because the focusing length decreases as the periodicity *a* and *b* increases. The equivalent refractive index increases as the periodicity *a* and *b* increases.

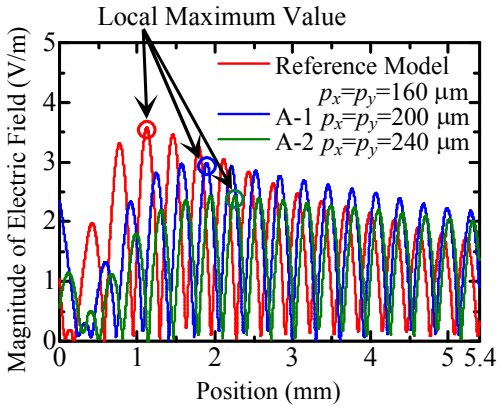

(a) Pattern A

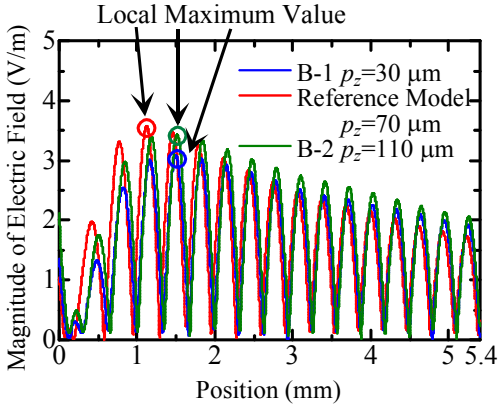

(b) Pattern B

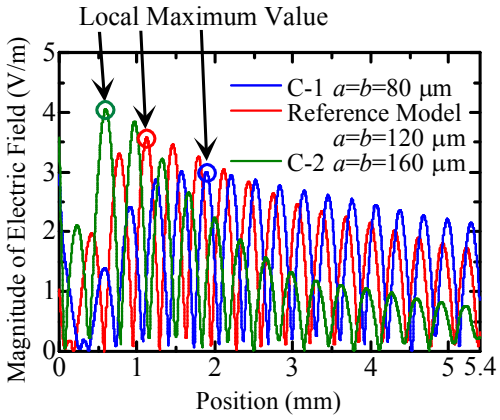

(c) Pattern C

Figure 9: Electric field.

5. Conclusions

This paper presents the focusing effect of an artificial dielectric lens that consist of metallic rectangular chips in the terahertz wave band and an explanation of the focusing length using a periodic analysis model. The periodic model analyses confirm the phase delay, and the full model analyses confirm the focus effect. The full model analysis confirms that the focusing length is longer with the larger periodicity of rectangular metal chips along the direction transverse to the propagation direction. It also confirms a nonuniform change for the periodicity along the propagation direction and a longer focusing length with narrower rectangular chips. The periodic model analysis can be used for iterative design of the refractive index for artificial dielectric lens with metallic rectangular chips, even under nonuniform changes with parameters. We are planning to fabricate the lenses and measure the focusing effect and the equivalent refractive index.

Acknowledgements

This research was supported by the Ministry of Education, Science, Sports and Culture, Grant-in-Aid for Scientific Research on Innovative Areas under Grant No. 23109505, Adaptable and Seamless Technology Transfer Program through Target-driven R&D, Japan Science and Technology Agency No. AS231Z04696B, and aid for scientific research from Takayanagi Memorial Foundation.

References

[1] W. E. Kock, "Metallic delay lenses," Bell Syst. Tech. J., vol. 27, no. 1, pp. 58-82, Jan. 1948.

[2] S. S. D. Jones, and J. Brown, "Metallic delay lenses," Nature, vol. 163, pp. 324-325, Feb. 1949.

[3] J. Brown, "The design of metallic delay dielectrics," Proceedings of the IEE - Part III: Radio and Communication Engineering, vol. 97, no. 45, pp. 45-48, Jan. 1950.

[4] S. B. Cohn, "Microwave measurements on metallic delay media," Proceedings of the IRE, vol. 41, no. 9, pp. 1177-1183, Sep. 1953.

[5] J. Brown, W. Jackson, "The relative permittivity of tetragonal arrays of perfectly conducting thin discs," vol. 102, no. 1, pp. 37-42, Jan. 1955.

[6] W. E. Kock, "Metal-lens Antennas," Proceedings of the I. R. E. and Waves and Electrons, vol. 34, no. 11, pp. 828-836, Nov. 1946.

[7] N. I. Landy, S. Sajuyigbe, J. J. Mock, D. R. Smith, and W. J. Padilla, "Perfect metamaterial absorber," Phys. Rev. Lett., vol. 100, pp. 207402-1-207402-4, May 2008.

[8] H. Tao, N. I. Landy, C. M. Bingham, X. Zhang, R. D. Averitt, W. J. Padilla, "A metamaterial absorber for the terahertz regime: design, fabrication and characterization," Opt. Express, vol. 16, no. 10, pp. 7181-7188, May 2008.

[9] H. Tao, C. M. Bingham, A. C. Strikwerda, D. Pilon, D. Shrekenhamer, N. I. Landy, K. Fan, X. Zhang, W. J. Padilla, and R. D. Averitt, "Highly flexible wide angle of incidence terahertz metamaterial absorber: Design, fabrication, and characterization," Phys. Rev. B, vol. 78, pp. 241103-1-241103-4, Dec. 2008.

[10] N. I. Landy, C. M. Bingham, T. Tyler, N. Jokerst, D. R. Smith, and W. J. Padilla, "Design, theory, and measurement of a polarization-insensitive absorber for terahertz imaging," Phys. Rev. B, vol. 79, pp. 125104-1-125104-6, Mar. 2009.

[11] H.-T. Chen, J. Zhou, J. F. O'Hara, F. Chen, A. K. Azad, and A. J. Taylor, "Antireflection coating using metamaterials and identification of its mechanism," Phys. Rev. Lett., vol. 105, pp. 073901-1-073901-4, Aug. 2010.

[12] M. Choi, S. H. Lee, Y. Kim, S. B. Kang, J. Shin, M. H. Kwak, K.-Y. Kang, Y.-H. Lee, N. Park and B. Min, "A terahertz metamaterial with unnaturally high refractive index," Nature, vol. 470, pp. 369-374, Feb. 2011.

[13] F. Miyamaru, M. W. Takeda, and K. Taima, "Characterization of terahertz metamaterials fabricated on flexible plastic films: toward fabrication of bulk metamaterials in terahertz region," Appl. Phys. Express, vol. 2, pp. 042001-1-042001-3, Mar. 2009.

[14] F. Miyamaru, S. Kubota, K. Taima, K. Takano, M. Hangyo, and M. W. Takeda, "Three-dimensional bulk metamaterials operating in the terahertz range", Appl. Phys. Lett., vol. 96, pp. 081105-1-081105-3, Feb. 2010.

[15] K. Sakakibara, J. Hirokawa, M. Ando, and N. Goto, "Periodic Boundary Condition for Evaluation of External Mutual Couplings in a Slotted Waveguide Array," IEICE Trans. Commun., vol.E79-B, no.8, pp.1156-1164, Aug. 1996..

[16] C. A. Balanis, *Antenna Theory*: *Analysis and Design* (3rd edition), John Wiley & Sons, 2005, sec. 4. 7. 1.